Parameter and State Estimation in Power Electronic Circuits

Linda A. Kamas, *Student Member, IEEE,* and Seth R. Sanders, *Member, IEEE*

Abstract— **Techniques for reconstructing or estimating unmeasured circuit variables and parameters in power electronic circuits are investigated. In numerous applications in power electronic systems, measurements of circuit variables are required for closed-loop control purposes or for diagnostic purposes, but are expensive or impossible to obtain directly. Examples are certain inductor currents, voltages at high impedance nodes where probes cannot be applied, or circuit variables in electrically isolated portions of a circuit. The method for state estimation relies on observer theory and is based on an intrinsic Lyapunov function, termed the *energy in the increment*. For cases where circuit parameters are not completely known, an adaptive estimation algorithm is developed for estimating the unknown circuit parameters along with the unmeasured circuit variables. The exponential stability of the combined parameter and state estimation scheme is established using averaging and singular perturbation analysis. Averaging analysis is used in off-line calculations to determine the feasibility of estimating certain parameters and to determine a basis from which to choose parameter update gains. Examples with an up–down converter illustrate the results. A hardware implementation of the state estimation scheme is also documented along with a description of a hardware implementation for parameter estimation.**

I. Introduction

TECHNIQUES for reconstructing or estimating unmeasured circuit variables and parameters in power electronic circuits are investigated here. In numerous applications in power electronic systems, measurements of circuit variables are required for closed-loop control purposes or for diagnostic purposes, but are expensive or impossible to obtain directly. Examples are certain inductor currents, voltages at high impedance nodes where probes cannot be applied, or circuit variables in electrically isolated portions of a circuit. One such example occurs in the application note [1]. In this application, an observer-like auxiliary circuit is used for output voltage estimation in a flyback converter. The auxiliary circuit, implemented with a few passive components and a tertiary transformer winding, is used to preserve electrical isolation between the primary and secondary sides of the power circuit. With this implementation, the error between the actual output voltage and the observer output is sensitive to the load current. The example developed in the present paper addresses this application, but relies on an adaptive estimation technique to reduce sensitivity to load current and other parameter variations.

The approach taken in this paper is based on observer theory [2], [3], and so the resulting algorithms may be implemented in real time. A natural scheme for implementing an observer with a circuit is given here. Some previous work on parameter and circuit waveform estimation for power circuits was based on off-line computational algorithms [4].

The paper is organized as follows. Some background on switching converters is given in Section II. Section III briefly reviews observer theory and introduces an approach for observer design for switching power circuits. The case considered in Section III is applicable only to the situation where circuit parameters are *known*. Since this is typically not the case in practice, Section IV extends the method to the situation where the circuit contains unknown parameters. In particular, Section IV develops an adaptive estimation algorithm for estimating unknown circuit parameters along with unmeasured circuit variables. A stability proof incorporating both the state and parameter estimation schemes is given in Section V. Section VI shows numerical calculations based on averaging analyses which provide a quick way to determine the viability of estimating different combinations of parameters. The schematic and observer waveforms for a hardware implementation of the state estimator is given in Section VII. Also in that section is a suggestion for hardware implementation of the combined parameter and state estimation scheme. An up–down converter is used as a vehicle throughout the paper to illustrate the results. Appendix A contains a discussion of the case where nonlinear resistive elements are present in the circuit. Appendix B contains the derivations for the averaging calculations presented in Section VI.

The *energy in the increment idea* was first presented for controllers in [5], [6]. This paper illustrates the use of the energy in the increment as a Lypaunov function in observers. This second application was first presented in [7].

II. Background Information

This section gives a brief background on dc-dc switching converters. To get a better understanding of the concepts behind switching converters, consider the model of an isolated up–down converter in Fig. 1. This circuit has two topologies, depending upon the switch position u. When $u = 0$, current does not flow from the source through the primary; thus the current in the mutual inductance flows through the "ideal" transformer and the diode turns on. With current flowing around the secondary loop that includes the diode, the ca-

Manuscript received February 19, 1992; revised December 3, 1992, and April 24, 1993. This work was supported by a grant from Tandem Computers and the UC MICRO Program. This paper was recommended by Associate Editor F. Y. Chang.

The authors are with the Department of Electrical Engineering and Computer Science, University of California, Berkeley, CA 94720.

IEEE Log Number 9211956.

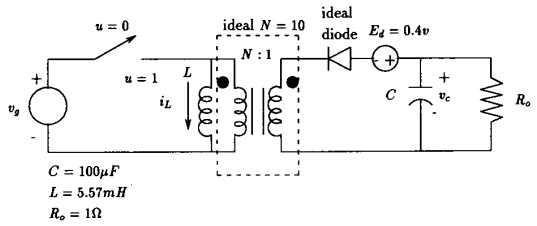

Fig. 1. Model of an isolated up–down converter.

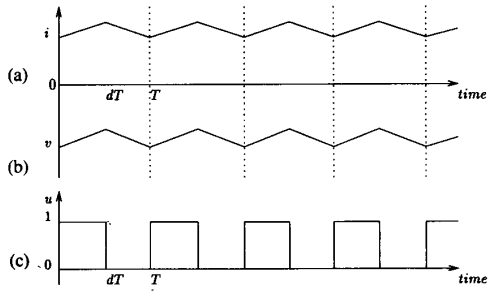

Fig. 2. (a) Magnetizing current. (b) Output voltage. (c) Switch position.

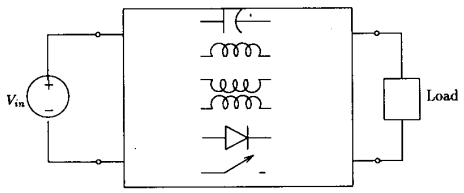

Fig. 3. General converter.

pacitor is charged until the next cycle. When $u = 1$, current is allowed to flow from the source to the primary, thus back-biasing the diode and restricting the capacitor to discharge on the output loop. The current and voltage waveforms of Fig. 2 show the steady-state behavior of the magnetizing current and output voltage for over four cycles. In general, we can view a dc-dc switching converter as a circuit with the structure of Fig. 3. The "box" consists of ideally lossless power processing circuitry built from transformers, inductors, capacitors, ideal diodes, and ideal switches.

Specifically, the converter of Fig. 1 has the state-space description

$$\dot{x} = Ax + (Bx + b)u + f \tag{1}$$

$$y = C(u)x + D(u) \tag{2}$$

where

$$A = \begin{bmatrix} 0 & \frac{N}{L} \\ -\frac{N}{C} & -\frac{1}{R_0 C} \end{bmatrix}, \quad B = \begin{bmatrix} 0 & -\frac{N}{L} \\ \frac{N}{C} & 0 \end{bmatrix}$$

$$b = \begin{bmatrix} \frac{V_g}{L} + \frac{NE_d}{L} \\ 0 \end{bmatrix}, \quad f = \begin{bmatrix} -\frac{NE_d}{L} \\ 0 \end{bmatrix}$$

$$C(u) = \begin{bmatrix} u & 0 \\ 0 & (1-u)N \end{bmatrix},$$

$$D(u) = \begin{bmatrix} 0 \\ uV_g - (1-u)NE_d \end{bmatrix}.$$

The variable x represents the two-component state vector composed of the inductor current and the capacitor voltage, u takes on the value 0 or the value 1 depending upon the instantaneous switch position, and y contains measurements of the transformer primary current and voltage. Note that all dependence on time t is suppressed in the notation. Typically the duty ratio d, the percentage of time in a switching period where $u = 1$, is determined by a control low of the form $d = g(x)$. For the purpose of this investigation, we shall consider open-loop operation, typically with $d = 0.5$. For more details and information on other types of converters, see [8].

III. State Estimation

In the case where all parameter values are known, the first step in constructing a state observer for the system (1) is to construct a system that exactly copies the dynamics of this system. Such a system would take the form

$$\dot{z} = Az + (Bz + b)u + f \tag{3}$$

where the vector z is an estimate of the state vector x. It is essential that the observer state z asymptotically converge to the underlying system state x. In order to study this behavior, one needs to examine the error dynamics that govern the error $e = z - x$, i.e.,

$$\dot{e} = Ae + uBe. \tag{4}$$

Since this dynamics may not in general be guaranteed to be stable or may not result in useful estimates in the presence of disturbances, observer theory leads one to incorporate a prediction error term formed from the difference between the measurement y of the output in (2) and the predicted output $C(u)z + D(u)$. The observer is then completed by injecting a signal proportional to the prediction error into the right-hand side of (3), yielding the observer system

$$\dot{z} = Az + (Bz + b)u + f + K(t)[C(u)z + D(u) - y] \tag{5}$$

with the associated error dynamics

$$\dot{e} = Ae + uBe + K(t)C(u)e. \tag{6}$$

A standard result of linear system theory [2], [3] guarantees that one can find a $K(t)$ that stabilizes this dynamics provided the system modeled by (1) and (2) is observable. (The form for one choice of $K(t)$ is illustrated in the specific example of Section 3.1.) For a switching-converter observer, where u is known at each time instant, the system is linear and time varying. Thus, we determine observability by checking that the observability Grammian [2], [3] of the system representation is positive definite. For any particular trajectory, this could be difficult to calculate, but for periodic steady-state operation, we can examine the form of the Grammian over one period to check observability. We can also check that varying the duty ratio will not affect the positive definiteness. In the example considered, we have determined that the system is observable for any nominal steady-state operation.

It turns out that the open-loop error dynamics (4) is asymptotically stable for the example of Fig. 1. Furthermore, there is

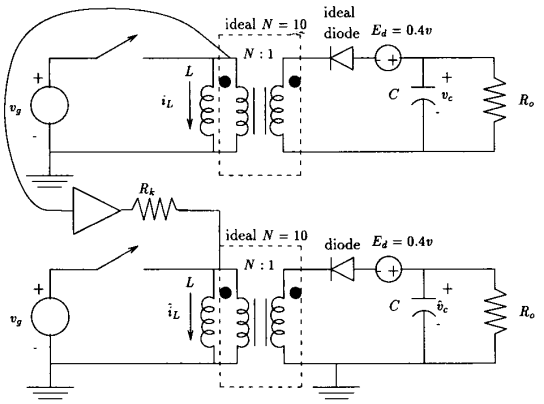

Fig. 4. Observer implementation scheme for up–down converter.

a natural Lyapunov function for this error dynamics given by

$$V(e) = \frac{1}{2}e^{\mathrm{T}}Qe$$
$$Q = \begin{bmatrix} L & 0 \\ 0 & C \end{bmatrix} \tag{7}$$

where the superscript T indicates the transpose of the associated vector. This function corresponds to the energy in the increment between the trajectories of the observer system and the trajectories of the underlying up–down converter. See Sanders [5] and Sanders and Verghese [6] for more details on the nature of this Lyapunov function and its use in exhibiting open-loop stability of switching power converters. Results in [5], [6] guarantee that the energy in the increment is a Lyapunov function for a power electronic circuit that is built from linear passive reactive elements, ideal switches, time-varying sources, and incrementally passive resistive elements. One conclusion for such a circuit is that any pair of trajectories corresponding to differing initial conditions cannot diverge. Since the open-loop observer and the underlying converter system correspond to identical dynamical systems that may be initialized with different initial conditions, we obtain

$$\dot{V}(e) = \frac{1}{2}\{e^{\mathrm{T}}[QA + A^{\mathrm{T}}Q]e + ue^{\mathrm{T}}[QB + B^{\mathrm{T}}Q]e\} \leq 0. \tag{8}$$

Furthermore, due to lossiness within the circuit, we essentially have $\dot{V}(e) < 0$. We conclude that the observer error, measured by $V(e)$, cannot increase.

3.1. Example: Up–Down Converter

A simulation of an open-loop observer has been carried out for the example up–down converter of Fig. 1. The results are shown in Fig. 5. Note that the convergence of the error can be slow and is actually controlled by the open-loop circuit dynamics.

It is possible to improve upon the open-loop observer by incorporating a prediction error gain of the form $K(u) = -Q^{-1}C^{\mathrm{T}}(u)R(u)$, where $R(u)$ is a positive semidefinite matrix for $u = 0, 1$. This gain results in the error dynamics

$$\dot{e} = Ae + uBe - Q^{-1}C^{\mathrm{T}}(u)R(u)C(u)e. \tag{9}$$

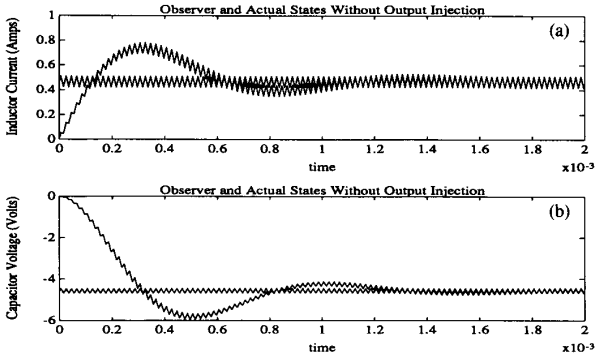

Fig. 5. Simulation of up–down open-loop observer. (a) Actual and observer currents. (b) Actual and observer voltages.

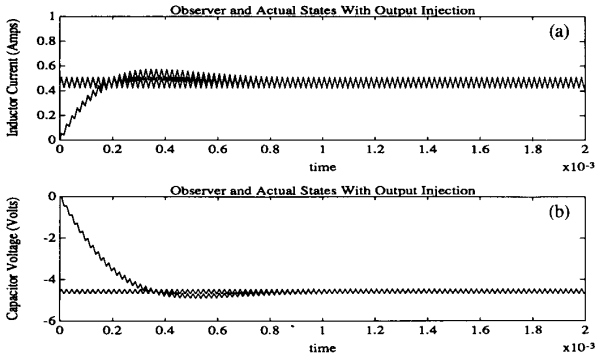

Fig. 6. Simulation with observer of up–down converter using prediction error. (a) Actual and observer currents. (b) Actual and observer voltages.

Differentiating the Lyapunov function (7) along this error dynamics yields

$$\dot{V}(e) = \tfrac{1}{2}\{e^{\mathrm{T}}[QA + A^{\mathrm{T}}Q]e + ue^{\mathrm{T}}[QB + B^{\mathrm{T}}Q]e - 2e^{\mathrm{T}}C^{\mathrm{T}}(u)R(u)C(u)e\} \leq 0. \tag{10}$$

In practice, we could select $R(u)$ to yield relatively fast *averaged* error dynamics controlled by the eigenvalues of $A + d_nB - Q^{-1}\overline{C^{\mathrm{T}}RC}$, where d_n is the nominal (constant) duty ratio and $\overline{C^{\mathrm{T}}RC}$ is the averaged value of the matrix $C^{\mathrm{T}}(u)R(u)C(u)$. Other criteria for the selection of R could be based on minimization of steady state errors due to parameter uncertainty or due to noise entering the system dynamics and the measurement equations [9]. Note that the observer with this form of prediction error gain can be implemented in a natural way as illustrated in Fig. 4 for the example up–down converter with electrical isolation. In order to preserve isolation, measurements are only taken from the high side of the isolation transformer. The circuit corresponds to a copy of the up–down converter with the prediction error injection implemented by a single resistor. For simplicity in this example, we have only used the measurement of the primary transformer voltage which corresponds to a singular matrix R. Note that all impedances could be scaled so that the observer has reduced currents and/or reduced voltages, compared to those of the underlying circuit. A simulation of waveforms obtained with this observer is shown in Fig. 6. Note that the errors converge more rapidly towards zero.

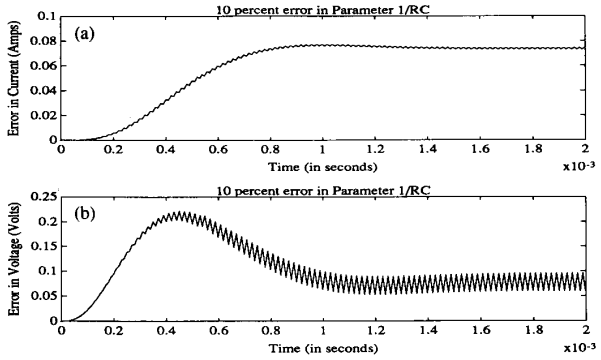

Fig. 7. Observer waveforms with parameter uncertainty. (a) Observer current error. (b) Observer voltage error.

It turns out that the approach taken in this section for constructing observers can be extended to the case where nonlinear resistive elements are present in the converter circuit. The only requirement is that these resistive elements be incrementally passive. An example of a power electronic circuit with such a nonlinear resistive element is a dc-dc converter operating in the discontinuous conduction mode. Appendix A gives details on this case.

IV. Parameter Estimation

The development in the previous section assumed that all circuit parameters were known a priori. To study the effects of unknown parameter values, the observer was simulated when the load resistance was perturbed by 10%. The results are shown in Fig. 7. One of the most notable features of this simulation is that there is a steady state bias in the state estimates produced by the observer: a 15% error in the current and a 2% error in the voltage.

A natural approach for dealing with this problem is to construct an adaptive observer that estimates the unknown circuit parameters along with the circuit state variables. In the sequel, we assume that the switch variable u is known for all time and that the portion of the measurement equation (2) that involves the state is exact; that is, the matrix $C(u)$ is known. However, we relax the assumption that the circuit parameters appearing in the state-space model (1) and in $D(u)$ in (2) are known. For the purposes here, define

$$A(u) = A + uB \tag{11}$$

$$b(u) = bu + f \tag{12}$$

so that the model (1) can be rewritten in the form

$$\dot{x} = A(u)x + b(u). \tag{13}$$

Since the parameters of this model are not precisely known, a first step in constructing an observer would be to use the best known estimates of the unknown parameters. The observer system corresponding to (5) could then take the form

$$\dot{z} = \hat{A}(u)z + \hat{b}(u) \tag{14}$$

where $\hat{A}(u)$ and $\hat{b}(u)$ are the available estimates of $A(u)$ and $b(u)$, respectively. We could introduce an error injection term to speed up convergence, but this is not done to keep the presentation simple. Note that the measurements will be used to update estimates for the parameters in the system model. The observer error $e = z - x$ is now governed by

$$\dot{e} = A(u)e + \delta A(u)z + \delta b(u) \tag{15}$$

where $\delta A(u) = \hat{A}(u) - A(u)$ and $\delta b(u) = \hat{b}(u) - b(u)$. It is generally possible to parameterize the circuit in a manner such that

$$A(u)x + b(u) = W(x, u)\theta^* \tag{16}$$

where $W(x, u)$ is a known matrix (depending on x and u) and all the unknown parameter information is contained in the vector θ^*. The important feature of this choice is that it is a *linear* parameterization. With this parameterization, the error equation (15) becomes

$$\dot{e} = A(u)e + W(z, u)\phi \tag{17}$$

where $\phi = \theta - \theta^*$ is a vector of differences between parameter estimates and actual parameter values, i.e., it is a vector of parameter errors. The solution of (17) is given by

$$e(t) = \Phi(t, t_0)e(t_0) + \int_{t_0}^{t} \Phi(t, \sigma)W(z(\sigma), u(\sigma))\phi \, d\sigma \tag{18}$$

where $\Phi(t, \sigma)$ is the state transition matrix corresponding to the system matrix $A(u)$. The corresponding error in the output $\delta y = C(u)(z - x) + \delta D(u)$ satisfies

$$\delta y = C(u)\left[\Phi(t, t_0)e(t_0) + \int_{t_0}^{t} \Phi(t, \sigma)W(z(\sigma), u(\sigma))\phi \, d\sigma\right] + \delta D(u). \tag{19}$$

The vector $\delta D(u)$ can also be expressed in the form $W_1(u)\phi$, where $W_1(u)$ is known. Assuming that the parameter update is *slowly varying* to the extent that it is essentially constant compared to the current and voltage dynamics, we can approximate (19) by taking the ϕ term outside the integral. (See Section V for a justification of this.) One then finds

$$\delta y = C(u)\Phi(t, t_0)e(t_0) + H(t)\phi \tag{20}$$

where $H(t) = C(u)\int_{t_0}^{t} \Phi(t, \sigma)W(z(\sigma), u(\sigma)) \, d\sigma + W_1(u)$, provided ϕ is constant. Noting that the term $\Phi(t, t_0)e(t_0)$ asymptotically decays to zero, we are led to attempt a parameter update law based on the gradient algorithm [10]. Such an algorithm takes the form

$$\dot{\theta} = -\epsilon H^{\mathrm{T}}\delta y \tag{21}$$

where $\epsilon \in R_+^1$ (R_+^1 = the set of positive real scalars) is a gain parameter. In practice, the system matrix $A(u)$ is unknown, so we instead use the available estimate of this matrix $\hat{A}(u)$ to construct an estimate $\hat{H}(t)$ of $H(t)$ via

$$\hat{H}(t) = C(u)\int_{t_0}^{t} \hat{\Phi}(t, \sigma)W(z(\sigma), u(\sigma)) \, d\sigma + W_1(u) \tag{22}$$

where $\hat{\Phi}(t, \sigma)$ is the state transition matrix that corresponds to the system matrix $\hat{A}(u)$. Note that $\hat{H}(t)$ converges to $H(t)$

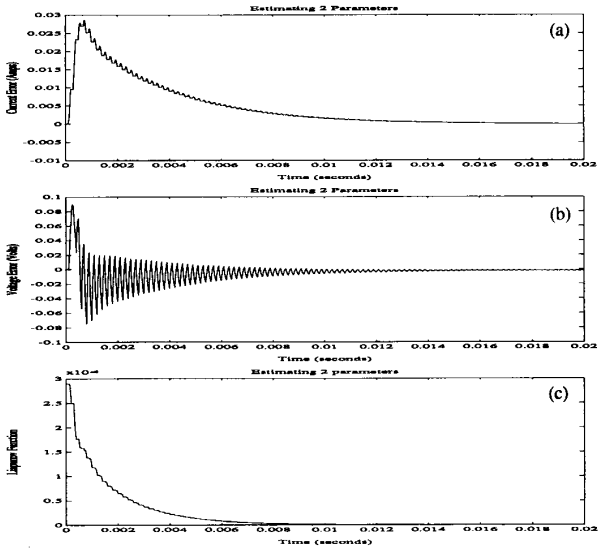

Fig. 8. Adaptive observer waveforms. (a) Error in current estimate. (b) Error in voltage estimate. (c) Lyapunov function ($V = 10^{-1}\phi_1^2 + 10^{-9}\phi_2^2$).

if the unknown system parameters converge to their actual values. The error in the parameter vector is then governed by the approximate dynamics

$$\frac{d}{dt}\phi \approx -\epsilon \hat{H}(t)^{\mathrm{T}} H(t)\phi \tag{23}$$

for slowly varying ϕ. For this analysis to hold, the gain ϵ needs to be selected so that the parameter update dynamics (23) evolve much more slowly than the observer error dynamics.

The convergence of the parameter error system can be studied via averaging analysis [10]. In particular, for a sufficiently small gain ϵ, the error dynamics are known to be exponentially stable if the *averaged* error dynamics are exponentially stable. One can therefore consider the stability properties of the averaged dynamics

$$\frac{d}{dt}\phi \approx -\epsilon \overline{\hat{H}(t)^{\mathrm{T}} H(t)}\phi \tag{24}$$

to assess the stability of the parameter error system. Details on an averaging analysis are given in Section V.

4.1. Example: Up–Down Converter

Here we illustrate the algorithm on our example up–down converter. For purposes of illustration, we assume that all parameters, except the load resistance and the diode forward voltage drop, are known, and hence the adaptive observer is designed to estimate these parameters along with the circuit state variables. The results of a simulation are shown in Fig. 8. Note that in this example, the estimator would allow one to avoid all measurements of secondary side circuit variables.

V. Stability

Here we study the stability of the system with combined parameter and state estimation schemes using singular perturbation techniques [11]–[13].

The state of the system with the combined parameter and state estimation schemes is $[\phi(t), e(t)]^{\mathrm{T}}$, where $\phi = \theta - \theta^*$ is the parameter estimation error; and $e = z - x$ is the state estimation error. The system is described by the following state equation:

$$\dot{\phi} = -\epsilon \hat{H}^{\mathrm{T}} C(u) e \tag{25}$$

$$\dot{e} = W(z, u)\phi + A(u)e \tag{26}$$

where $\hat{H}(t) = C(u)[\int_{t_0}^{t} \hat{\Phi}(t, 0) W(z, u)\, d\sigma]$. Notice that the variable ϕ is considered to be slowly varying compared to the variable e since we have chosen ϵ to be appropriately small. We are dealing with systems where $\dot{e} = A(u(t))e$ is exponentially stable. To transform these equations into a form suitable for singular perturbation analysis, we rescale time by setting $\tau = t\epsilon$. Then,

$$\frac{d\phi}{dt} = \frac{d\phi}{d\tau}\frac{d\tau}{dt} = \frac{d\phi}{d\tau}\epsilon$$

which results in the following:

$$\frac{d\phi}{d\tau} = -\hat{H}^{\mathrm{T}}(\tau) C(u) e(\tau) \tag{27}$$

$$\epsilon \frac{de}{d\tau} = W(z(\tau), u(\tau))\phi(\tau) + A(u(\tau))e(\tau). \tag{28}$$

We further transform the system to an approximately upper block-triangular form by using the similarity transformation:

$$\begin{bmatrix} \phi(\tau) \\ \eta(\tau) \end{bmatrix} = \begin{bmatrix} I_p & 0 \\ -L(\tau) & I_n \end{bmatrix} \begin{bmatrix} \phi(\tau) \\ e(\tau) \end{bmatrix} \tag{29}$$

where $L(\tau) = \int_{\tau_0}^{\tau} \Phi_\epsilon(\tau, \sigma)(1/\epsilon) W(z, u)\, d\sigma$. We explain this choice in the following.

Recall that the error trajectory is described by

$$e(\tau) = \Phi_\epsilon(\tau, \tau_0) e(\tau_0) + \int_{\tau_0}^{\tau} \Phi_\epsilon(\tau, \sigma) \frac{1}{\epsilon} W(z, u)\phi(\sigma)\, d\sigma \tag{30}$$

where $\Phi_\epsilon(\tau, \tau_0)$ is the state transition matrix of the system $\epsilon(dx/d\tau)x = A(u(\tau))x$. With the assumption that the parameter update scheme is slowly varying compared to the speed of the circuit state dynamics, we approximate (30) by

$$\xi(\tau) = \Phi_\epsilon(\tau, \tau_0)\xi(\tau_0) + \int_{\tau_0}^{\tau} \Phi_\epsilon(\tau, \sigma) \frac{1}{\epsilon} W(z, u)\, d\sigma\, \phi(t). \tag{31}$$

Thus, we have defined $\eta(\tau) = e(\tau) - \xi(\tau)$ to be the difference between the true error trajectory and the singularly perturbed ($\epsilon = 0$) approximation to it. With $L(\tau) = \int_{\tau_0}^{\tau} \Phi_\epsilon(\tau, \sigma)(1/\epsilon) W(z, u)\, d\sigma$, we have $\eta(\tau) = e(\tau) - L(\tau)\phi(\tau)$. Note that in the new time scale, $H(\tau) = C(u)[\int_{\tau_0}^{\tau} \Phi_\epsilon(\tau, \sigma)(1/\epsilon) W(z, u)\, d\sigma] = C(u)L(\tau)$. The similarity transformation results in

$$\frac{d\phi}{d\tau} = -\hat{H}^{\mathrm{T}} H\phi - \hat{H}^{\mathrm{T}} C\eta \tag{32}$$

$$\epsilon \frac{d\eta}{d\tau} = A_{2,1}(\tau)\phi + [A(u(\tau)) + \epsilon L \hat{H}^{\mathrm{T}} C]\eta \tag{33}$$

where

$$A_{2,1}(\tau) = -\epsilon\frac{dL(\tau)}{d\tau} + A(u)L(\tau) + W(z, u) + \epsilon L(\tau)\hat{H}^{\mathrm{T}}CL(\tau) \quad (34)$$

$$= \epsilon L\hat{H}^{\mathrm{T}}H. \quad (35)$$

In this case, $L(\tau)$ is the zero state solution of

$$\epsilon\frac{dL(\tau)}{d\tau} = A(u)L(\tau) + W(z, u) \quad (36)$$

which is a first-order approximation of

$$\epsilon\frac{dL_{\mathrm{tot}}(\tau, \epsilon)}{d\tau} = A(u)L_{\mathrm{tot}}(\tau, \epsilon) + W(z, u) + \epsilon L_{\mathrm{tot}}(\tau, \epsilon)\hat{H}^{\mathrm{T}}CL_{\mathrm{tot}}(\tau, \epsilon). \quad (37)$$

Note that if the solution, $L_{\mathrm{tot}}(\tau, \epsilon)$, of (37) were used in place of $L(\tau)$ in (29), then $A_{2,1}(\tau) = 0$ and the system (32)–(33) would be upper block triangular. A method such as this was used for a stable linear time-invariant system with slow parameter update in [13]. Using analysis similar to that in [13], it can be shown that the solution of (37) is an ϵ-perturbation of the solution of (36) (i.e., that $L_{\mathrm{tot}}(\tau, \epsilon) = L(\tau) + \epsilon L_1(\tau, \epsilon)$, where $L(\tau)$ is the solution of (36) and $L_{\mathrm{tot}}(\tau, \epsilon)$ is the solution of (37)). The stability analysis would then involve ensuring bounds on ϵ in conjunction with bounds on $L_1(\tau, \epsilon)$.

The following stability analysis uses $L(\tau)$, the solution of (36), and only looks to bounds on ϵ for stability, simplifying the analysis. Equations (32)–(33) can be rearranged into the form

$$\begin{bmatrix} \epsilon\frac{d\phi(\tau)}{d\tau} \\ \epsilon\frac{d\eta(\tau)}{d\tau} \end{bmatrix} = \begin{bmatrix} -\epsilon\hat{H}^{\mathrm{T}}H & -\epsilon\hat{H}^{\mathrm{T}}C \\ 0 & A(u) \end{bmatrix}\begin{bmatrix}\phi \\ \eta\end{bmatrix} + \begin{bmatrix} 0 & 0 \\ \epsilon L\hat{H}^{\mathrm{T}}H & \epsilon L\hat{H}^{\mathrm{T}}C \end{bmatrix}\begin{bmatrix}\phi \\ \eta\end{bmatrix}. \quad (38)$$

The system (38) can be viewed in light of the averaging analysis for two-time scale systems developed in [10]. Using this analysis, a result in [10, p. 185] shows exponential stability for the equilibrium point $\phi = 0, \eta = 0$ with ϵ sufficiently small by showing $\phi = 0$ to be an exponentially stable equilibrium point of the averaged system $d\phi_{\mathrm{av}}/d\tau = -(\hat{H}^{\mathrm{T}}H)_{\mathrm{av}}\phi_{\mathrm{av}}$. The analysis requires uniform exponential stability of $\epsilon(d\eta/d\tau) = A(u)\eta$, which holds in the cases of the power circuits under consideration. Exponential stability of the averaged system is shown in Section VI, assuming initial parameter errors are small.

In summary, the combined parameter and state estimation scheme is exponentially stable if the averaged "slow" system is exponentially stable, the fast system dynamics are uniformly exponentially stable, and the parameter update is sufficiently slowly-varying (ϵ is sufficiently small).

VI. Averaging Analysis

The averaging analysis will be done in two parts: 1) stability analysis of $\dot{\phi}_{\mathrm{av}} = (\hat{H}^{\mathrm{T}}H)_{\mathrm{av}}\phi_{\mathrm{av}}$, and 2) calculation of $(H^{\mathrm{T}}H)_{\mathrm{av}}$.

6.1. Exponential Stability of the Averaged System

Consider the Lyapunov function candidate for the averaged system:

$$V = \phi_{\mathrm{av}}^{\mathrm{T}}\phi_{\mathrm{av}}. \quad (39)$$

Differentiating V along the averaged system trajectory, one finds

$$\dot{V} = \dot{\phi}_{\mathrm{av}}^{\mathrm{T}}\phi_{\mathrm{av}} + \phi_{\mathrm{av}}^{\mathrm{T}}\dot{\phi}_{\mathrm{av}} \quad (40)$$

$$= -\phi_{\mathrm{av}}^{\mathrm{T}}(H^{\mathrm{T}}H)_{\mathrm{av}}\phi_{\mathrm{av}} - \phi_{\mathrm{av}}^{\mathrm{T}}[H^{\mathrm{T}}(\delta H) + (\delta H)^{\mathrm{T}}H]_{\mathrm{av}}\phi_{\mathrm{av}} \quad (41)$$

where $\delta H = \hat{H} - H$. Note that $(H^{\mathrm{T}}H)_{\mathrm{av}}$ is positive definite assuming H satisfies a persistency of excitation (P.E.) condition [10]. From (41), $\dot{V}$ is negative as long as the matrix norm of $(H^{\mathrm{T}}(\delta H) + (\delta H^{\mathrm{T}})H)_{\mathrm{av}}$ does not exceed $\lambda_{\min}((H^{\mathrm{T}}H)_{\mathrm{av}})$, where $\lambda_{\min}$ is the smallest eigenvalue of $(H^{\mathrm{T}}H)_{\mathrm{av}}$. In this case,

$$\dot{V} \le -\lambda_{\min}((H^{\mathrm{T}}H)_{\mathrm{av}})V + \left\|(H^{\mathrm{T}}(\delta H) + (\delta H^{\mathrm{T}})H)_{\mathrm{av}}\right\|V \quad (42)$$

which implies that the averaged system is exponentially stable with rate greater than or equal to

$$\frac{1}{2}[\lambda_{\min}((H^{\mathrm{T}}H)_{\mathrm{av}}) - \left\|(H^{\mathrm{T}}(\delta H) + (\delta H^{\mathrm{T}})H)_{\mathrm{av}}\right\|].$$

We can analyze this further to find a *sufficient* condition for stability with a bound on the variation of H:

$$\lambda_{\min}((H^{\mathrm{T}}H)_{\mathrm{av}}) \ge 2k_1k_2 \ge \frac{2}{T}\int_0^T \|\delta H\|\,\|H\|\,dt \quad (43)$$

where $k_1 = \|\delta H\|$ and $k_2 = \|H\|$. This is a conservative bound and in practice may not be very useful other than as a simple first check. If $\lambda_{\min}((H^{\mathrm{T}}H)_{\mathrm{av}})$ is small, one needs to ensure that the initial estimates of parameter values are sufficiently close to the actual values. Theoretically, the analysis shows that there exists some region around zero parameter error for which small perturbations of the parameters can be corrected by this adaptive estimation scheme.

6.2. Calculation of $(H^{\mathrm{T}}H)_{\mathrm{av}}$

The main purpose of the following discussion is to study the feasibility of estimating various parameter combinations from various measurement combinations. This is achieved by showing how one would calculate $(H^{\mathrm{T}}H)_{\mathrm{av}}$ and then looking at its condition number. Different parameter and measurement combinations enter the calculation through the W and C matrices and result in different condition numbers for $(H^{\mathrm{T}}H)_{\mathrm{av}}$. A well-conditioned matrix implies that estimation of the selected parameters would be practical with the given measurements.

The theoretical derivation for computing $(H^{\mathrm{T}}H)_{\mathrm{av}}$ are in Appendix B. The following section gives the numerical results and interpretation.

6.2.1. Numerical Calculations: Calculations of $(H^{\mathrm{T}}H)_{\mathrm{av}}$ using MATLAB for the up–down converter were done assuming current and voltage measurements were taken on the primary side of the transformer. Of course, the conditioning for a system with one unknown parameter is perfect, i.e., the condition number is 1. In this case, it is still useful to do the averaging calculation in that the value of $(H^{\mathrm{T}}H)_{\mathrm{av}}$ is like an eigenvalue of the parameter update system and gives an idea of how to choose the parameter update gain. For example, in estimating the single parameter $1/R_0C$, $(H^{\mathrm{T}}H)_{\mathrm{av}}$ turns out to be -5.56×10^{-7}, but the eigenvalues of the converter system (using state-space averaging [8]) are around -5000. Thus a gain of $\epsilon = 10^7$ would not be considered to be large.

In estimating the two parameters E_d and $1/R_0C$, the condition number of $(H^{\mathrm{T}}H)_{\mathrm{av}}$ was moderately large at 9.67×10^{10}, but since simulations were done in MATLAB, with 16 digit accuracy, it was certainly possible to estimate these two parameters in simulations (see Section IV). However, convergence was sped up by increasing the switching period T tenfold in order to get more excitations into the system. This is reflected in calculations of $(H^{\mathrm{T}}H)_{\mathrm{av}}$ with a tenfold larger switching period, resulting in a condition number of 3×10^9. The averaging calculation yielded

$$(H^{\mathrm{T}}H)_{\mathrm{av}} = \begin{bmatrix} 1.12 \times 10^3 & -0.0131 \\ -0.0131 & 5.56 \times 10^{-7} \end{bmatrix}$$

whose eigenvalues are 1×10^3 and 4×10^{-7}. This implies that part of the system could be converging much faster than the other part. To compensate for this, we could generalize our scalar gain ϵ to a positive definite matrix gain,

$$G = \begin{bmatrix} \epsilon_{1,1} & \epsilon_{1,2} \\ \epsilon_{1,2} & \epsilon_{2,2} \end{bmatrix}.$$

For instance, we could start with $\epsilon_{1,1} = 0.1$, $\epsilon_{2,2} = 10^7$, and $\epsilon_{1,2} = 0$ in order to even out the parameter convergence. Thus, the averaging calculation provides a basis from which to begin choosing gains.

Not surprisingly, $(H^{\mathrm{T}}H)_{\mathrm{av}}$ was poorly conditioned when trying to estimate more than two parameters. For example, in estimating the three parameters N/C, N/L, and $1/R_0C$, the condition number of $(H^{\mathrm{T}}H)_{\mathrm{av}}$ is 7.6×10^{18}. One might conclude that it is not reasonable to try to estimate three parameters of this system using only the two primary-side measurements.

6.2.2 Comments: An inherent feature of our averaging analysis is that it used the average steady-state values of the states in the calculation of W which in turn was used in $(H^{\mathrm{T}}H)_{\mathrm{av}}$. Thus we ignored any excitation in W, other than the dc component, that may have contributed to the persistency of excitation in H as a whole. Thus, all excitation generated was a result of the switching action between A_0 and A_1, and not the "input" term W, which was held constant. This makes the averaging analysis somewhat conservative. Although approximate, the averaging analysis simplified matters to an extent where quick calculations could be made to get a good basic understanding of the limits to the parameter identification method developed in Section IV.

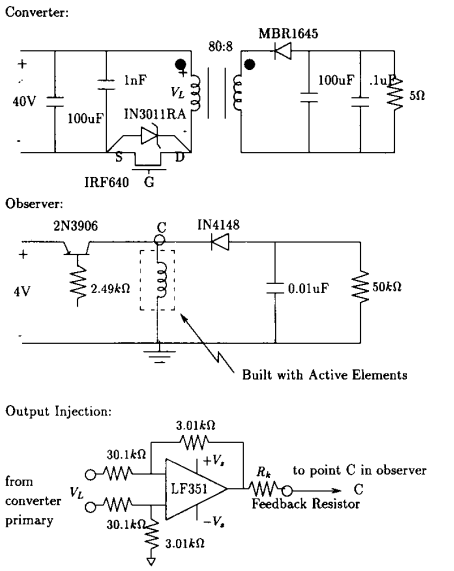

Fig. 9. Hardware implementation.

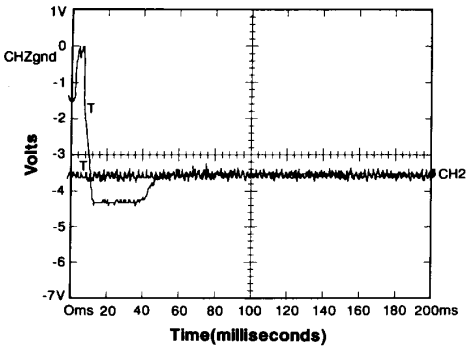

Fig. 10. Output voltages of converter and open-loop observer.

VII. Hardware Implementation

This section is divided into two sections. Section 7.1 describes a hardware implementation of the state observer for the up–down converter and shows the resultant waveforms. Section 7.2 describes a possible hardware implementation for the parameter update scheme.

7.1. State Observer

The observer scheme for the up–down converter was implemented in hardware according to the schematic in Fig. 9. This does not include the parameter estimation scheme. Note that for the observer circuit, the inductor was implemented with active elements. Also, the "turns ratio" and element values of the observer were scaled differently than in the original circuit. The switching frequency was 30 kHz.

The most useful feature of the waveforms was the steady-state average, to which it was possible for the observer voltage to converge, without output injection. Fig. 10 shows an open-loop observer start-up transient. The waveform corresponds

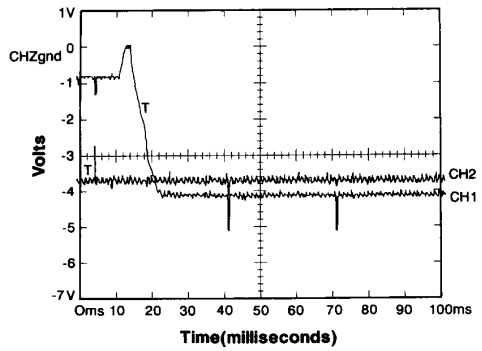

Fig. 11. Output voltages of converter and observer with 221Ω feedback resistance.

to the converter output voltage. When output injection was implemented, the resulting transient behavior was faster, but a small steady-state error appeared in the observer waveform. Typical waveforms of the converter and observer voltages with feedback resistance of 221Ω are shown in Fig. 11.

7.2. Parameter Update Scheme

The parameter update scheme of Section IV also lends itself to hardware implementation. This is easiest to see in the construction of the matrix $\hat{H}(t)$, reprinted here:

$$\hat{H}(t) = C(u)\int_{t_0}^{t} \hat{\Phi}(t, \tau)W(z(\tau), u(\tau))\, d\tau + W_1(u). \quad (44)$$

The matrix $\hat{H}(t)$ is obtained from the system equation

$$\frac{d}{dt}L(t) = \hat{A}(u(t))L(t) + W(z(t), u(t)) \quad (45)$$

$$\hat{H}(t) = C(u)L(t) + W_1(z(t), u(t)). \quad (46)$$

To calculate $\hat{H}(t)$, this system could be implemented as a set of circuits, each with the same structure as the observer circuit. There would be one circuit for each parameter, i.e., column of $W(z, u)$. The sources in each circuit would correspond to the elements of each column of $W(z, u)$. The resulting implementation would realize the calculation of the sensitivity in the output y to variations of the parameter vector ϕ. For more details on sensitivity calculation, see [14].

VIII. Conclusions and Direction of Further Study

In this paper we have developed techniques for estimating power electronic circuit waveforms and parameters using only a limited set of measurements. The given example, an isolated up–down converter, illustrated that it is possible to implement these schemes with measurements taken from only one side of the transformer, preserving isolation. Simulation results verified the theoretical development of the state and parameter estimation schemes. The state estimation scheme was also verified by a hardware implementation.

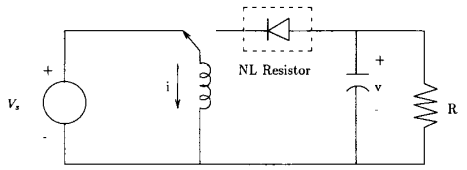

Fig. 12. Up–down converter model for discontinuous conduction mode.

A. The Case of Nonlinear Resistive Elements

In the case where nonlinear resistive elements are present in a power circuit, the state-space model can be recast as

$$Q\dot{x} = -(1-u)\mathcal{H}_0(x) - u\mathcal{H}_1(x) \quad (47)$$

$$y = C(u)x + D(u) \quad (48)$$

where x is the vector of inductor currents and capacitor voltages, Q is the matrix of inductances and capacitances, and $\mathcal{H}_i(\cdot)$ are hybrid representations for the nonreactive portion of the circuit that correspond to each of the switch configurations. A consequence of the incremental passivity of the resistive elements is that the hybrid representations are also incrementally passive, i.e.,

$$(z-x)^{\mathrm{T}}[\mathcal{H}_i(z) - \mathcal{H}_i(x)] \geq 0 \quad (49)$$

for any x and z and for $i = 0, 1$. An observer for the system modeled by (47)–(48) can then take the form:

$$Q\dot{z} = -(1-u)\mathcal{H}_0(z) - u\mathcal{H}_1(z) + K(u)[C(u)z + D(u) - y]. \quad (50)$$

A choice of $K(u) = C(u)^{\mathrm{T}}R(u)$ with $R(u)$ positive semidefinite will then result in stable error dynamics, obtained by subtracting (47) from (50). This can be demonstrated by differentiating the energy in the increment $V = \frac{1}{2}(z-x)^{\mathrm{T}}Q(z-x)$ along trajectories of the error system. Carrying out this procedure, we find

$$\begin{aligned}\dot{V} = &-(1-u)(z-x)^{\mathrm{T}}[\mathcal{H}_0(z) - \mathcal{H}_0(x)] \\ &- u(z-x)^{\mathrm{T}}[\mathcal{H}_1(z) - \mathcal{H}_1(x)] \\ &- (z-x)^{\mathrm{T}}C(u)^{\mathrm{T}}R(u)C(u)(z-x). \end{aligned} \quad (51)$$

The first two terms on the right-hand side of (51) are nonpositive as a result of the incremental passivity of the resistive elements in the circuit, while the third term is nonpositive by design. The conclusion is that the error dynamics are stable. Asymptotic stability can typically be obtained in practice. A nontrivial example of a circuit containing such a nonlinear resistive element is a converter operating in discontinuous conduction mode. Fig. 12 shows a model of an up–down converter containing an ideal single-pole double-throw switch and an ideal diode that prevents the inductor current from reversing. In the discontinuous conduction mode, the diode can be viewed as a nonlinear incrementally passive resistive element. As such, it is possible to construct an observer for this circuit using the framework of this paper.

B. Derivation of $(H^{\mathrm{T}}H)_{\mathrm{av}}$

Here we derive the equations of the averaged system. Because we assume that the parameter update is slowly varying compared to the state and error dynamics, we calculate and use the average value of the steady-state trajectory. In relation to the slow system, the fast system is oscillating so fast that the only thing the fast system "sees" is the steady-state average. For simplicity, we use $(x_{\mathrm{ss}})_{\mathrm{av}}$ instead of $(z_{\mathrm{ss}})_{\mathrm{av}}$, $\delta y = 0$, and $u_{\mathrm{av}} = d$ in the regressor calculation. The steady-state value of x at the beginning of a cycle is determined by setting $x_{\mathrm{ss}}(t_0 + T) = x_{\mathrm{ss}}(t_0)$, resulting in

$$x_{\mathrm{ss}}(t_0) = (I - e^{A_1\bar{d}T}e^{A_0dT})^{-1}\left[e^{A_1\bar{d}T}\int_{t_0}^{t_0+dT} e^{A_0(t_0+dT-\tau)}\,d\tau + \int_{t_0+dT}^{t_0+T} e^{A_1(t_0+T-\tau)}\,d\tau\right]Bv \quad (52)$$

where $\bar{d} = (1 - d)$, A_0 is the system matrix while $t_0 \le t < (t_0 + dT)$, and A_1 is the system matrix while $t_0 + dT \le t < (t_0 + T)$. Since the calculations get more complicated from here, then without loss of generality, we will set $t_0 = 0$ to simplify notation. Averaging over one period of the steady-state response, we obtain

$$x_{\mathrm{SSav}} = \frac{1}{T}\left[\int_0^{dT}\left(e^{A_0t}x_{0\mathrm{ss}} + \int_0^t e^{A_0(t-\tau)}\,d\tau Bv\right)dt + \int_{dT}^{T}\left(e^{A_1(t-dT)}x_{dT\mathrm{ss}} + \int_{dT}^t e^{A_1(t-\tau)}\,d\tau Bv\right)dt\right] \quad (53)$$

where $x_{0\mathrm{ss}} = x_{\mathrm{ss}}(0)$, $x_{dT\mathrm{ss}} = x_{\mathrm{ss}}(dT)$. Since the state-transition matrix of the L system is the same as that for the converter, we obtain

$$\overline{L}_{0\mathrm{ss}} = (I - e^{A_1\bar{d}T}e^{A_0dT})^{-1}\left[e^{A_1\bar{d}T}\int_{t_0}^{t_0+dT} e^{A_0(t_0+dT-\tau)} + \int_{t_0+dT}^{t_0+T} e^{A_1(t_0+T-\tau)}\,d\tau\right]W(x_{\mathrm{av}}, 0, d) \quad (54)$$

where $\overline{L}(t) = \Phi(t, 0)\overline{L}_0 + \int_{t_0}^t \Phi(t, \tau)W(z, \delta y, u)\,d\tau$. Now we calculate the average by

$$H(t) = C\left[e^{A_0t}\overline{L}_{0\mathrm{ss}} + \int_0^t e^{A_0(t-\tau)}\,d\tau W\right], \quad 0 \le t < dT \quad (55)$$

$$H(t) = C\left[e^{A_1(t-dT)}\overline{L}_{dT\mathrm{ss}} + \int_{dT}^t e^{A_1(t-\tau)}\,d\tau W\right], \quad dT \le t < T \quad (56)$$

$$H_0(t) = H^{\mathrm{T}}(t)H(t), \qquad 0 \le t < dT \quad (57)$$

$$H_1(t) = H^{\mathrm{T}}(t)H(t), \qquad dT \le t < T \quad (58)$$

$$(H^{\mathrm{T}}(t)H(t))_{\mathrm{av}} = \frac{1}{T}\left[\int_0^{dT} H_0(t)\,dt + \int_{dT}^{T} H_1(t)\,dt\right]. \quad (59)$$

REFERENCES

[1] Power Integrations, Inc., Mountain View, CA, "Power integrated circuit databook," 1992, application note AN-8.
[2] C. Desoer, "Course notes for linear systems (221A)," Univ. of California, Berkeley, 1989.
[3] T. Kailath, *Linear Systems.* Englewood Cliffs, NJ: Prentice-Hall, 1980.
[4] M. Kudisch, G. Verghese, and J. Lang, "Off-line parameter and state estimation for power electronic circuits," in *PESC Rec.*, 1988, pp. 509–516.
[5] S. Sanders, "Nonlinear control of switching power converters," Ph.D. dissertation, Dept. EECS, M.I.T., Cambridge, MA, Jan. 1989.
[6] S. Sanders and G. Verghese, "Lyapunov-based control for switched power converters," in *PESC Rec.*, 1990, pp. 51–58.
[7] L. Kamas and S. Sanders, "Parameter and state estimation of power electronic circuits," in *PESC Rec.*, 1991, pp. 57–61.
[8] J. Kassakian, M. Schlecht, and G. Verghese, *Principles of Power Electronics.* Reading, MA: Addison-Wesley, 1991.
[9] A. Gelb (Ed.), *Applied Optimal Estimation.* Cambridge, MA: MIT Press, 1974.
[10] S. Sastry and M. Bodson, *Adaptive Control: Stability, Convergence, and Robustness.* Englewood Cliffs, NJ: Prentice-Hall, 1989.
[11] P. Kokotovic, H. Khalil, and J. O'Reilly, *Singular Perturbation Methods in Control.* New York: Academic Press, 1986.
[12] P. Kokotovic, B. Riedle, and L. Praly, "On a stability criterion for continuous slow adaptation," *IEEE Syst. Contr. Lett.*, pp. 7–14, 1985.
[13] B. Anderson, R. Bitmead, C. Johnson, Jr., P. Kokotovic, R. Kosut, I. Mareels, L. Praly, and B. Riedle, *Stability of Adaptive Systems: Passivity and Averaging Analysis.* Cambridge, MA: M.I.T. Press, 1986.
[14] L. Chua and P. Lin, *Computer-Aided Analysis of Electronic Circuits.* Englewood Cliffs, NJ: Prentice-Hall, 1975.

Linda A. Kamas received the B.S. degree in electrical engineering from the University of California at Santa Barbara in 1988. She received the M.S. degree from the University of California at Berkeley in 1991, where she is currently working toward the Ph.D. degree in electrical engineering. Her research interests include systems and control theory, power electronics, and design of system reliability.

Seth R. Sanders received S.B. degrees in electrical engineering and physics from M.I.T., Cambridge, MA, in 1981. He then worked as a design engineer at the Honeywell Test Instrument Division in Denver, CO. He returned to M.I.T. in 1983 and received the S.M. and Ph.D. degrees in electrical engineering in 1985 and 1989, respectively.

He is presently an Assistant Professor in the Department of Electrical Engineering and Computer Sciences at the University of California, Berkeley. His research interests are in nonlinear circuits and systems, and particularly in applications to power electronic and electromechanical systems. During the 1992–1993 academic year, he was on industrial leave with National Semiconductor in Santa Clara, CA.